AIMS Materials Science, 9(6): 863–883.
DOI: 10.3934/matersci.2022052
Received: 24 July 2022
Revised: 18 September 2022
Accepted: 20 October 2022
Published: 31 October 2022

http://www.aimspress.com/journal/Materials

Research article

Mechanical analyses of flat sheet water treatment membranes

Murat Ozdemir[1], Selda Oterkus[1,*], Erkan Oterkus[1], Islam Amin[1,2], Abdel-Hameed El-Aassar[3] and Hosam Shawky[3]

[1] PeriDynamics Research Centre, Department of Naval Architecture, Ocean and Marine Engineering, University of Strathclyde, 100 Montrose Street, Glasgow G4 0LZ, UK
[2] Department of Naval Architecture and Marine Engineering, Port Said University, Port Said 42511, Egypt
[3] Egypt Desalination Research Centre of Excellence (EDRC) and Hydrogeochemistry Department, Desert Research Centre, Cairo 11753, Egypt

* **Correspondence:** Email: selda.oterkus@strath.ac.uk; Tel: +44-141-548-4979.

Abstract: In this work, we address the mechanical response of the flat sheet polymeric water treatment membranes under the assumed operational loading conditions. Firstly, we perform quasi-static analyses of the membranes under normal pressure loads, which is the condition that resembles the actual loading for flat sheet membranes in the submerged membrane bioreactors. Then, the long-term deformation of the membranes is studied under the assumed filtration durations for the same loading conditions by utilizing the viscoelastic material models. The quasi-static and viscoelastic membrane simulations are performed by a commercial finite element code ANSYS. Finally, the mechanical fatigue life predictions are carried out based on the stress distributions from the quasi-static analyses and the long-term effects from the viscoelastic analyses.

Keywords: mechanical analysis; flat sheet; water treatment; membrane; fatigue; viscoelasticity

1. Introduction

As the consequences of the climate change have been more evident in the recent decade, it is crucial to utilize the water resources effectively. These impacts are more severe for the societies in

geographically disadvantageous parts of the earth. In this regard, reuse of wastewater plays a prominent role in a sustainable water management. Among the water reuse applications, membrane bioreactors have a significant place [1]. Both organic and inorganic based materials can be adopted as the membrane materials; however, the organic based polymeric membranes are relatively popular thanks to their lower investment costs [2]. On the other hand, the polymeric membranes are vulnerable to mechanical degradation caused by harsh content of the feed water, backwashing as well as the chemical cleaning [3].

The structural integrity of the membranes holds a substantial importance for a reliable water filtration operation and so the public health and environmental considerations. Wang et al. [4] presented an extensive literature study, which covers useful techniques for the evaluation of mechanical characterization of membrane materials. Among them, the first method that comes to mind is the uniaxial tensile tests for the strength and stiffness evaluation of membrane materials. The parameters that can be obtained by the uniaxial tensile tests are: stress–strain curves, Young's modulus, yield stress, ultimate stress and elongation at break [4]. Ahmed et al. [5] studied the mechanical strength of (PVDF-HFP) composite flat sheet membranes for efficient oil-water separation process using standard dog-bone specimens. The uniaxial tests can also be employed for hollow fibre type membranes made up of either organic [6] or inorganic based materials [7]. Dynamic Mechanical Analysis (DMA) is another suitable technique to characterize the viscous behaviour of polymeric materials under various environmental conditions [8]. Viscous damping properties of the membranes can be determined by DMA under various temperature and test frequencies [9]. Though the uniaxial tensile tests for the mechanical response characterization of the membranes are relatively generic, the actual loading condition and the response of flat-sheet membranes can be resembled by the bursting tests [4]. Lalia et al. [10] investigated the mechanical properties of PVDF-HFP flat sheet membranes using the bursting tests.

To the best of authors' knowledge, the mechanical fatigue life prediction of water treatment membranes under filtration cycles has not been reported yet. This issue has also been reported in the review work of Wang et al. [4]. One of the similar works that can also be employed for the water treatment membrane was presented by Mackin et al. [11], which investigates the mechanical fatigue life of polymeric films under biaxial stress state using a spherical intender. Their experimental work was supported by the finite element (FE) analyses as well as the nonlinear membrane theory in [11].

Taking into account the lack of works on the fatigue life predictions of water treatment membranes in the open literature, we aim to present a general framework on the mechanical response analysis of flat-sheet water treatment membranes under realistic operational pressure loads. The main focus is given to fatigue life prediction; however, the viscoelastic creep deformation and its impact on the membrane performance are also to be addressed in the present work.

The outline of the present manuscript is established as follows. Section 2 is dedicated to description of case studies, evaluation of membrane material properties as well as the problem setup. The quasi-static analysis by Finite Element Method (FEM) are performed for filtration and backwashing pressure loads in Section 3.1. The viscoelastic analyses for the long term deformation prediction of the membranes under filtration are performed in Section 3.2. The stress and strain values obtained from the quasi-static and viscoelastic FE analyses are utilized for fatigue life predictions in Section 3.3. Finally, Section 4 presents the concluding remarks.

2. Materials and methods

In the membrane bioreactors, the flat-sheet membranes are compacted in cassette form, which includes the frames and spacers. The frame is the component that provides the structural integrity of the membrane module under filtration and backwashing pressure loads, while the spacers are utilised to lead permeate flow inside the membrane cassette for the hydrodynamic efficiency [12]. Apart from the hydrodynamic impact of the spacers, flat-sheet membranes are supported by the spacers especially under the filtration process. During the backwashing, the spacers will not have any structural support unless special arrangements are considered for membranes, see [13].

The membrane sheets with spacers are schematically illustrated in Figure 1. In the given figure, the cassette frame is not demonstrated for simplicity. The spacers are assumed to be fixed to cassette frame at the ends, so are the membrane sheets. The spacers also prevent the contact of the membranes with each other.

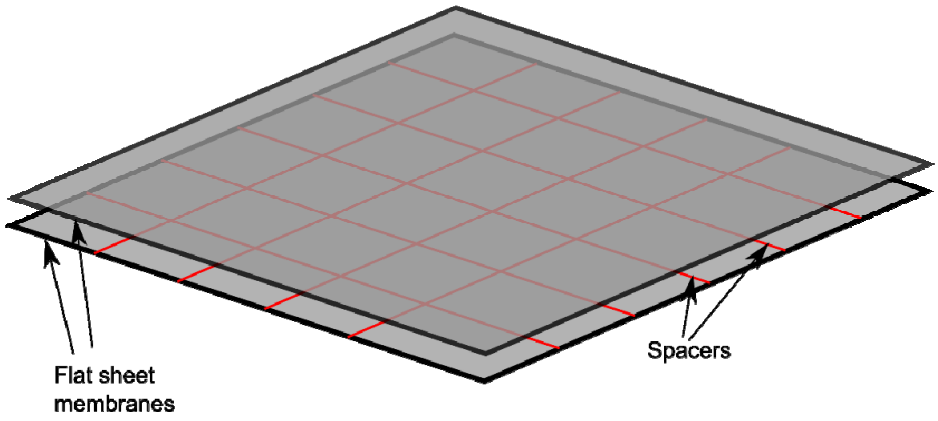

Figure 1. Flat sheet membrane model with spacers.

2.1. FE modeling

The membrane sheets are subjected to hydrostatic pressure in the submerged configuration; however, the driving force for the filtration is usually generated by the vacuum pressure on the permeate side of the bioreactor. Then, we will assume that the both sheets will be subjected to same pressure due to the main vacuum condition on the permeate side. The influence of the hydrostatic pressure change on the total pressure load can be omitted.

The vacuum pressure ideally sucks the membranes towards each other, and the contact of the membrane sheets is prevented by the spacers. This sucking condition is represented by the normal pressure on the membrane surfaces in the FE models. Moreover, the FE model can be simplified by modelling only one sheet with suitable boundary conditions (BCs). The representative model of the membrane and associated FE mesh are shown in Figure 2.

We will consider two different spacer configurations, which divide the membrane sheets into 10 × 10 and 20 × 20 sub-regions. The spacer configurations have been selected for illustrative purposes and they may have significant effect on the mechanical response. It is expected that the

spacers will support the membrane sheet under the filtration pressure. It is also noted that the design drive for the spacer configurations is usually the hydrodynamic performance [12]. The procedure, which shall be presented next is ideally applicable for any spacer configuration for the flat sheet membranes. Figure 2a demonstrates the case with the 10 × 10 sub-regions.

The principal dimensions of the membrane sheet will be kept same throughout the study, and they are assumed as $L \times W \times t_m = 500 \times 500 \times 2$ mm regardless of the spacer configuration. Here, the parameters stand for the length, width and thickness of the membrane sheet, respectively. The thickness of the membrane has been decided so that the membrane can withstand high pressure values with relative coarse spacer configurations (10×10 configuration); however, the procedure in the present work is applicable for any thickness of flat-sheet membranes.

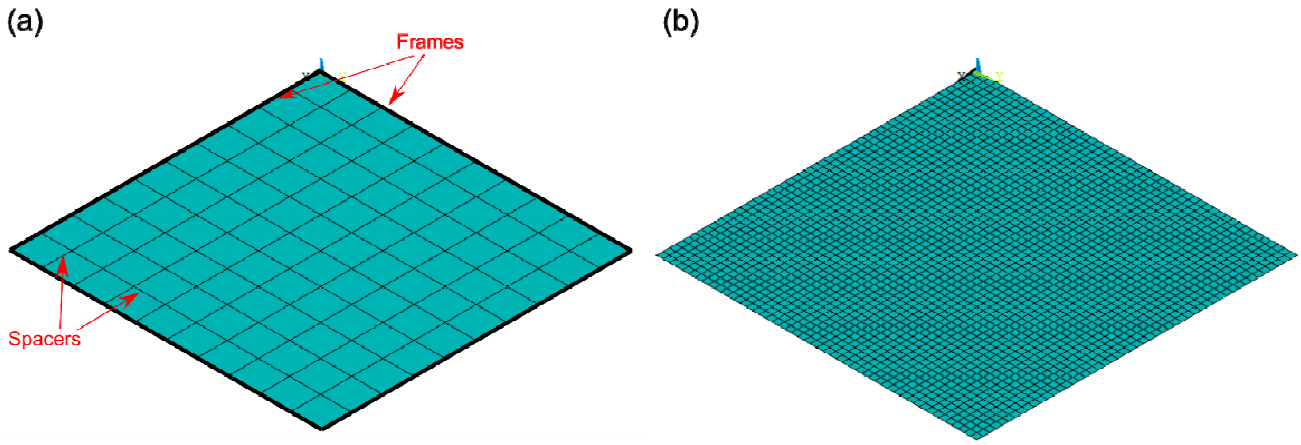

Figure 2. Simplified membrane modelling: (a) Representative membrane sheet model with spacers and framing, (b) FE mesh model of the membrane sheet.

2.1.1. Loading and BCs

As described in the preceding section, the load is applied as normal pressure on the membrane surfaces for both filtration and backwashing operation. In the implementation of the BCs, we make some assumptions that reflect the realistic condition with sufficient simplicity. The membrane's edges along the framing lines are assumed to be fixed, i.e., both translations and rotations of the membrane sheet are constrained along the edges.

The spacers are invoked in the FE models in a simplified manner to avoid computational burden and the possible numerical instabilities arising from multiple contact points, which might be the case if the spacer and membrane sheets are modelled separately and the contact conditions are introduced. So, the spacers are not modelled explicitly, but suitable BCs are introduced along the spacer lines as shown in Figure 2a. The boundary conditions for the spacers under filtration condition are as follows.

(*i*) The displacement component normal to the membrane surface is constrained.

(*ii*) The rotation component about the axis parallel to the spacer line is constrained.

The latter condition is a reasonable assumption since the suction condition will create

non-rotation region along the spacer lines under the real operation. On the other hand, if the backwashing is employed, the membrane sheet is supposed to deform outwards, and the spacers will have no support against membrane deformation. It is therefore assumed that the membrane sheets will deform freely under backwashing, and the BCs for spacers mentioned above are not applicable for the backwashing condition.

The load implementation is to be set regarding the requirements for a stable FE solution for both quasi-static and viscoelastic simulations. In the case of quasi-static analyses, the desired pressure load, either for filtration or backwashing case, is increased gradually until the desired value is attained. If the viscoelastic analysis is the case, the load has to be implemented and should be kept constant for a desired duration. In the FE framework, the viscoelastic analysis is essentially transient analysis without inertia effects.

In the transient analysis, the load can be applied in two ways: (i) ramped loading, (ii) stepped loading [14]. Stepped loading is ideal for the viscoelastic analysis since we aim to keep the load constant for a certain duration; however, the sudden implementation of loading may cause numerical difficulties because of the excessive deformation in some elements. In this regard, the pressure load is gradually increased until the desired pressure level in a relatively short amount of time, then the load magnitude is kept constant. The load implementation schemes for quasi-static and viscoelastic analyses are illustrated in Figure 3. In this figure, the time parameter in the quasi-static analyses is not the physical time and this is the reason for the term "Pseudo-time" in Figure 3a.

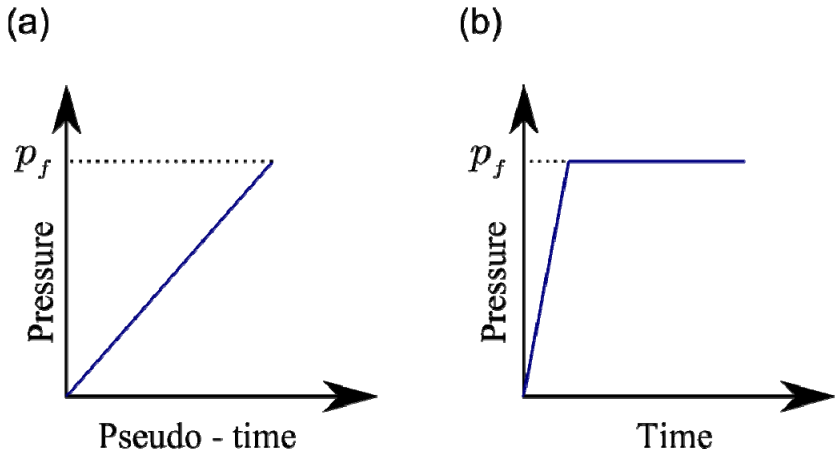

Figure 3. Load implementation schemes for: (a) Quasi-static analyses, (b) Viscoelastic analyses.

2.1.2. FE mesh and element properties

In the modelling of membrane sheets, we employ Shell181 elements in ANSYS package. Since we aim to perform viscoelastic analysis in addition to accurate stress results from a series of quasi-static analyses, full integration option of the stiffness matrix is adopted.

Mesh density is adjusted based on the spacer configuration. If the membrane sheet is divided into 10 × 10 sub-regions by the spacers, the number of elements between the spacer lines

(boundary of sub-regions) is set as five. As for the cases with 20 × 20 sub-regions, the number of elements between the spacer lines is set as three. The domain discretization for backwashing conditions is performed in the same manner so as to keep the number of nodes/elements consistent. Figure 2b shows the density of FE mesh for the 10 × 10 sub-regions case.

2.1.3. Evaluation of the material properties

The material properties are derived from the work of Emori et al. [15]. The reference work performs both experiments and FE calculations regarding the creep behaviour of the hollow fibre membranes involving 3D pore geometry. In the present work, we will assume that our membrane sheets are fabricated by the same material tested in [15].

The generic material properties are adopted from the tensile tests provided by [15]. The experimental stress-strain curve for the highest strain rate, i.e., $\dot{\varepsilon} = 1.4 \times 10^{-2}$ in [15], is digitized; then the Young's modulus and yield stress are derived from the digitized curve as $E = 138.9$ MPa and $\sigma_Y = 4.04$ MPa. With a reasonable approach, the approximate yield strain for the membrane material is calculated as $\varepsilon_Y = 0.029$. FE quasi-static analyses are performed by employing these material properties.

As far as the viscoelastic simulation is concerned, the time dependent material properties have to be introduced. In ANSYS FE code, the viscoelastic material properties can be represented by generalized Maxwell model comprised of Maxwell elements and a spring element, which are connected parallel to each other [16]. The relaxation of the viscoelastic material is mathematically represented by the Prony series, which have the exponential decay terms. The viscoelastic material properties are ideally provided by the relaxation of the shear modulus as expressed below by a Prony series expression.

$$G(t) = G_\infty + \sum_{i=1}^{N_M} G_i \times e^{(-t/\tau_i)} \tag{1}$$

In Eq 1, G_∞ denotes the shear modulus of the material when the time converges to infinity, which basically represents the elastic stiffness of the single spring element on the generalized Maxwell model. G_i is shear modulus of each Maxwell element, while the relaxation time of each Maxwell element is represented by τ_i. The number of Maxwell elements in the model is defined as N_M.

For the PVDF material tested in [15], the fundamental material properties are given previously in this section. The same material was tested under constant loads to capture the creep deformation in the same work [15]. We will take the results of the creep tests presented in the reference work to obtain the viscoelastic material properties. Here, it must be noted that the applied load at the creep tests should be below the elastic limits so that we can assume the membrane deformation comprises elastic and viscous parts but the plastic deformation does not occur. In this regard, we have chosen the creep test result for 3 N axial loading in Ref. [15]. This axial load corresponds to approximately 3.6 MPa axial stress, which is below the yielding point, and is sufficiently large to provide valuable creep data. Once the data provided for 3 N in Figure 4 of Ref. [15] is digitized, we can convert the

data to the relaxation of Young's modulus by a simple expression as:

$$E(t) = \frac{\sigma}{\varepsilon(t)} \tag{2}$$

Having the time-dependent Young's modulus readily leads us to evaluate the time dependent shear modulus. From that point, a nonlinear curve fitting tool can be employed to fit a curve in the form of Prony series to the discrete data. By taking two exponential terms ($N_M = 2$) in the Prony series, a curve is fitted to the discrete shear modulus data using the nonlinear curve fitting tool of MATLAB® [17].

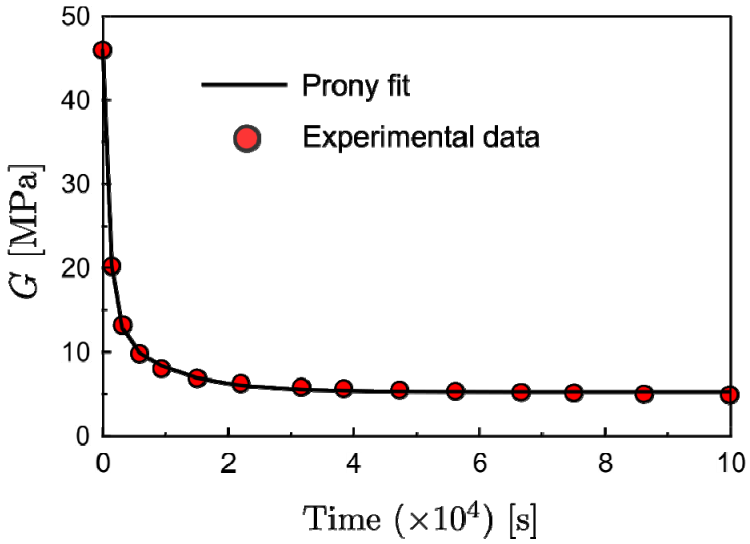

Figure 4. Prony series fit for the experimental shear modulus data.

The correlation between the discrete data and the fitted curve can be observed in Figure 4. The mathematical expression for the fitted curved is given as:

$$G(t) = 5.228 + 8.758 \times e^{(-t/0.906)} + 31.92 \times e^{(-t/0.103)} \tag{3}$$

The parameters in Eq 3 should be properly introduced to a FE code for the viscoelastic simulation.

2.2. Mechanical fatigue life calculations

The fatigue simulations aim to provide life predictions of the membranes under variable mechanical loads. The influence of the wear and corrosion of the membrane material are currently not taken into account. The loading procedure and one load cycle definition for the cases with and without backwashing implementation are given in Figures 5 and 6, respectively.

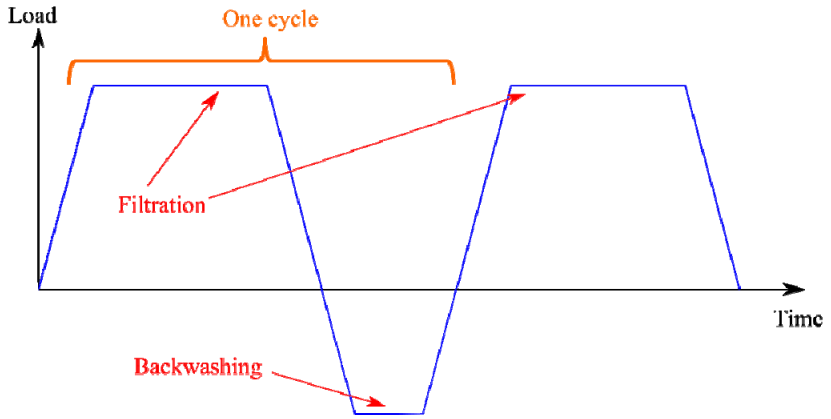

Figure 5. Loading procedure for filtration + backwashing cycle.

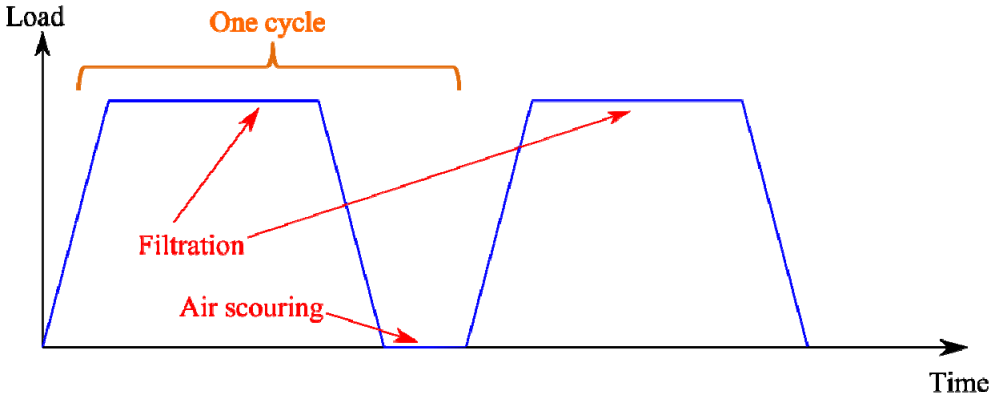

Figure 6. Loading procedure for filtration + air scouring cycle.

The duration of filtration is assumed as 2 h, while the duration of the backwashing and the air scouring is relatively short, i.e., 5 min. In this regard, the viscous effects are omitted for the backwashing process.

Since it is known that the backwashing process may compromise the structural integrity of flat sheet membranes, membrane fouling is usually controlled by membrane relaxation + air scouring. In this process, it is assumed that the membrane sheet is unloaded and the air scouring does not generate any significant stress on the membrane. The duration of membrane relaxation + air scouring is also taken as 5 min.

2.2.1. Fatigue life calculation procedure

We employ a simplified fatigue life prediction method, which takes into account the viscous deformation effects for filtration indirectly. The flowchart of fatigue life calculation procedure is presented in Figure 7.

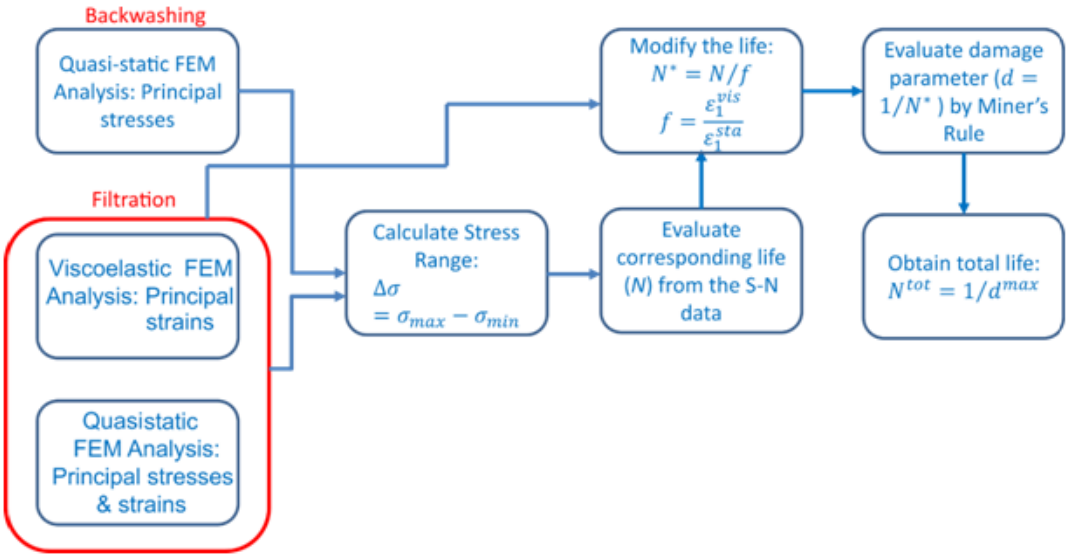

Figure 7. Fatigue life calculation procedure for the membrane sheets.

The process shown in Figure 7 is described as follows. First, we perform quasi-static analyses for the filtration process. Then, the viscoelastic analysis should be performed for predicting the long-term deformation of the membranes under filtration transmembrane pressure. Since the duration of backwashing is much shorter than the filtration, we can omit the long-term effects for backwashing. Then, only quasi-static analyses are performed for the membranes under backwashing pressure.

We will extract maximum principal stresses and strains from the FE simulations. The stress range will be calculated by the principal stresses from the quasi-static analyses of filtration and backwashing. Once the stress range is calculated, the corresponding life from the S-N data can be obtained. Then, this life should be modified for the long-term effects. A factoring coefficient is employed for the modification purposes, which is the ratio of long-term 1st principal strain to the 1st principal strain from the quasi-static analyses for filtration. Afterwards, fatigue damage parameter for each cycle is obtained by Miner's sum. Finally, the total number of cycles for the fatigue life of the membrane is obtained by relating it to the maximum damage parameter.

2.2.2. Miner's rule

The accumulation of the fatigue damage is obtained by the Miner's rule. Therefore, this method is briefly touched here. The total damage on a particular location can be expressed as:

$$D = \sum_i^k \frac{n_i}{N_i} \tag{4}$$

In Eq 4, D represents the total damage at a certain location. The number of loading cycles at that location for a certain stress range is denoted as n, while N is the corresponding total fatigue life at the given stress range obtained by the S-N data at hand. The total number of stress range blocks is represented by k. If the accumulated damage value, D becomes equal to 1.0 at any point in the

membrane sheet, it is assumed that the membrane fails due to the fatigue damage accumulation.

It is also important to note that the frequency of loading is neglected as it is too small because of the longer filtration periods. Furthermore, the mean stress correction is not considered either due to the lack of relevant data.

2.2.3. Fatigue properties

We aim to carry out fatigue life predictions based on the stress results obtained from the quasi-static FE simulations. Moreover, we will not consider any pre-existing damage/crack on the membrane sheets. In this regard, the fatigue life predictions are to be undertaken based on suitable S-N relations. To the best of authors' knowledge, the available material fatigue data on PVDF membrane materials are limited. Tng [18] presented some useful fatigue results for the hollow fibre membranes under cyclic tensile loading. In addition to that, Solvay [19] published a design and processing guide for PVDFs. When we digitize the S-N curve in [19], we have noticed that the coefficient C, in the $S = C \times N^{-m}$ form of expression, is slightly higher than the yield stress of the considered material. The slope coefficient is $m = 0.02$. By invoking this similarity between the coefficient C and the yield strength of the material, we assume a series of S-N curves for the PVDF membrane sheet material in the present work. The form of the S-N relation is taken as $S = C \times N^{-m}$. The parameter is C is utilized as slightly higher than the yield strength of the material as $C = 4.438$, and the inverse slope coefficients are varied as $m = 0.02, 0.04$ and 0.06 in the forthcoming fatigue calculations. The comparison of the S-N curves for varying m values but the same intersection point (C coefficient) with the vertical axis is provided in Figure 8.

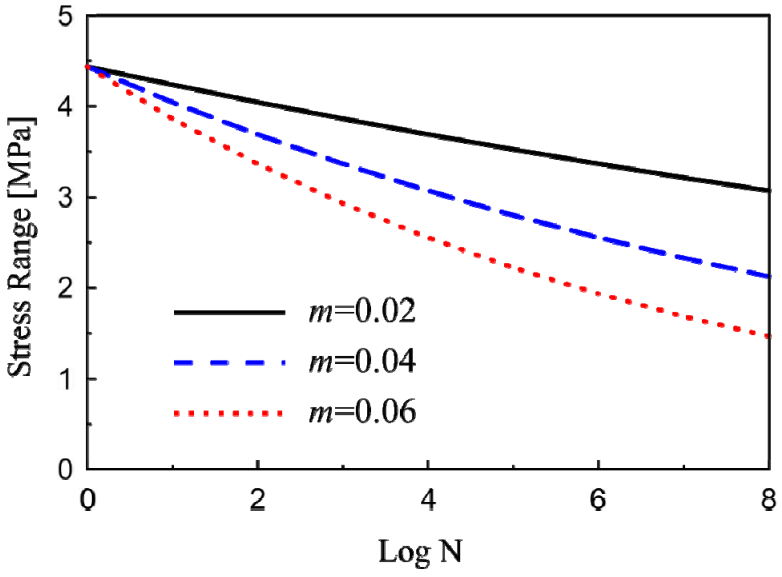

Figure 8. Comparison for S-N curves for varying *m* values.

It must be noted that the present S-N curve parameters are for the pristine material without any long-term corrosion and environmental effects. The S-N data for the membrane materials under corrosive environments have not been published in the open literature yet to the best of authors'

knowledge. However, the present fatigue life prediction procedure can be effectively adopted for the membranes under corrosive environments as long as the proper S-N curves representing the corrosion effects are adopted.

2.3. Test scenarios

In this section, we summarize all the parameters and test cases for the proposed fatigue life prediction and mechanical analysis procedures.

A single membrane sheet size is adopted in the present work as $L \times W \times t_m = 500 \times 500 \times 2.0$ mm. For the same size of the membrane, the spacer configurations are adjusted as 10×10 and 20×20. The change of the spacer configuration will impact the support conditions of the membrane sheet under the filtration process, while the load and support condition will remain same in the backwashing process for both spacer configurations.

The vacuum filtration pressures are taken as: $P_f = 0.5, 1.0, 1.5$ and 2.0 bar. These filtration pressures are applied as uniform surface pressures on the membrane sheets. Since flat sheet membranes are usually vulnerable to backwashing [20], we consider two different backwashing conditions: (i) 2 h of filtration without backwashing, (ii) 2 h of filtration with a gentle backwashing. The backwashing duration is practically several minutes. In the latter case, the backwashing pressure is set as $P_b = 0.1$ bar. In the first case, the fouling is to be controlled by the membrane relaxation and air scouring after filtration. At this point, it is assumed that the load variations acting on the membrane sheet due to the air scouring are insignificant and do not make any change in the loading condition for fatigue life prediction procedure.

As described in the material modelling section, we will vary the slope coefficient, *m*, in the fatigue life estimations for each loading configuration.

3. Results and discussion

3.1. Quasi-static FE analyses

The first step in the mechanical durability assessment of flat sheet water treatment membranes is the evaluation of stresses-strains and displacements under the static loading conditions. The results will reveal useful information by an immediate check if the membrane sheets fail under the given loads. More importantly, the stress results from these analyses will comprise the basis for the fatigue life predictions.

The equivalent stress distributions for $P_f = 0.5$ and 2.0 bar are given in Figure 9. The results for $P_f = 1.0$ and 1.5 bar will fall in between the results presented in this figure; we therefore have not given the stress results for these cases in Figure 9 to save the space. However, we have provided the maximum values of the equivalent and principal stresses in Figure 10 for all pressures.

The stress distributions in Figure 9 apparently demonstrate the spacer configurations' effects. Maximum equivalent stresses take place along the framing edge, which is the expected situation. In the quasi-static analyses, the membrane is assumed to be intact; however, the stress distributions on the membrane materials may show different patterns depending on degradation and localized damage

of the material in the long-term use.

The equivalent stress distribution and the displacement component normal to the membrane surface for the backwashing condition are given in Figure 11. In all loading and spacer configurations, the membrane sheet deforms below its elastic limits. One should pay attention to the deformation of the membrane in the backwashing condition. Under the considered backwashing pressure, $P_b = 0.1$ bar, the maximum normal displacement is around 37 mm, which is far above the membrane thickness. This large deformation also suggests that the pressure load is compensated by the in-plane forces; the influence of the bending deformations is small. Excessive deformation may cause the decline of permeate water quality in the long-term usage of the membranes. This issue will be discussed quantitatively in the next section.

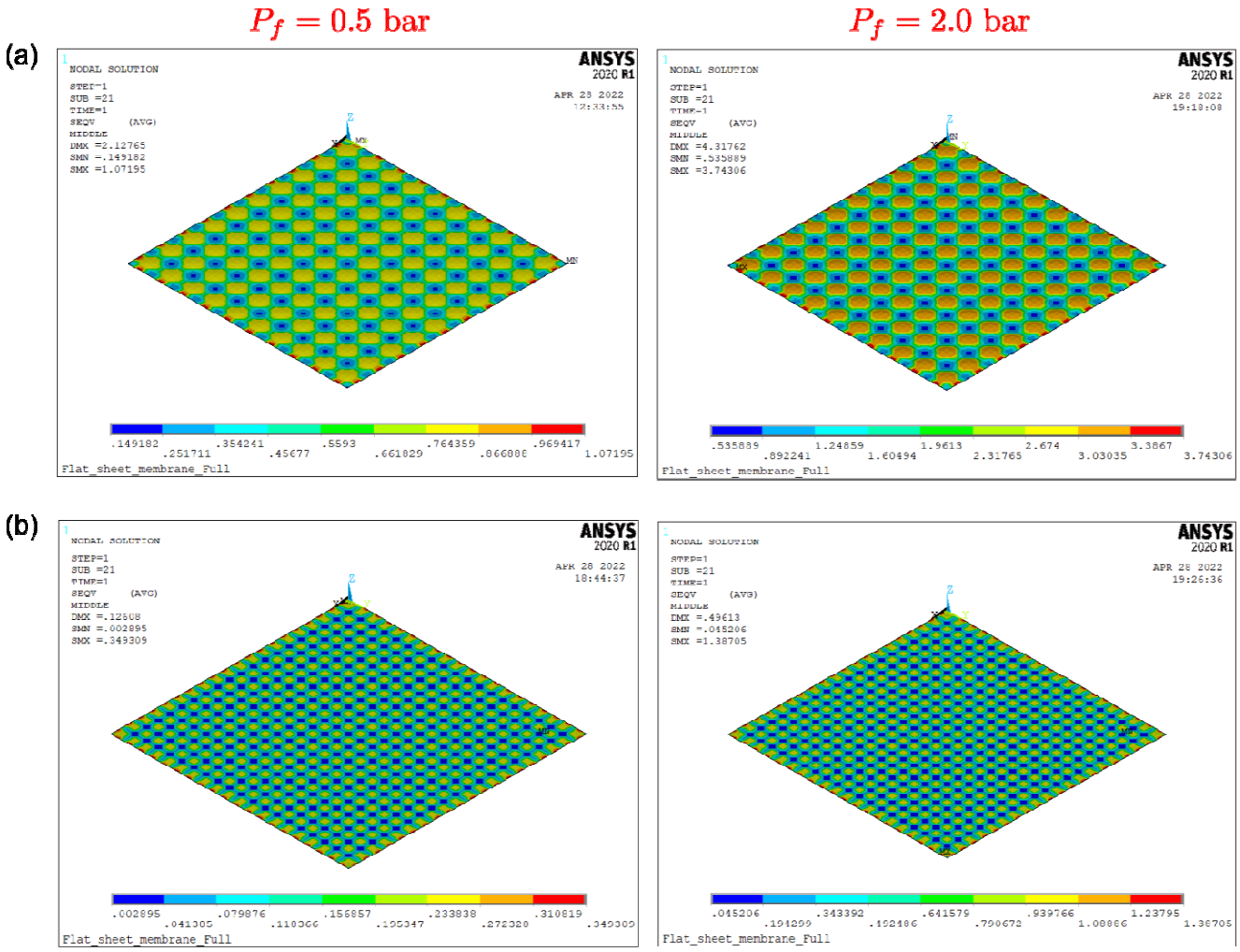

Figure 9. Equivalent (Von Mises) stress distribution (MPa): (a) 10×10 configuration, (b) 20×20 configuration.

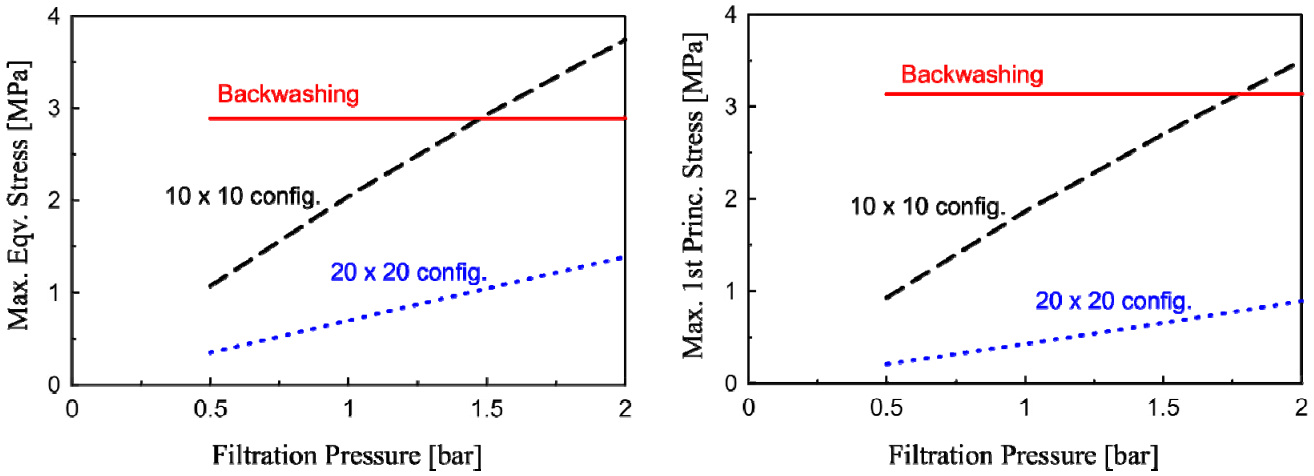

Figure 10. Maximum values of the main stress components.

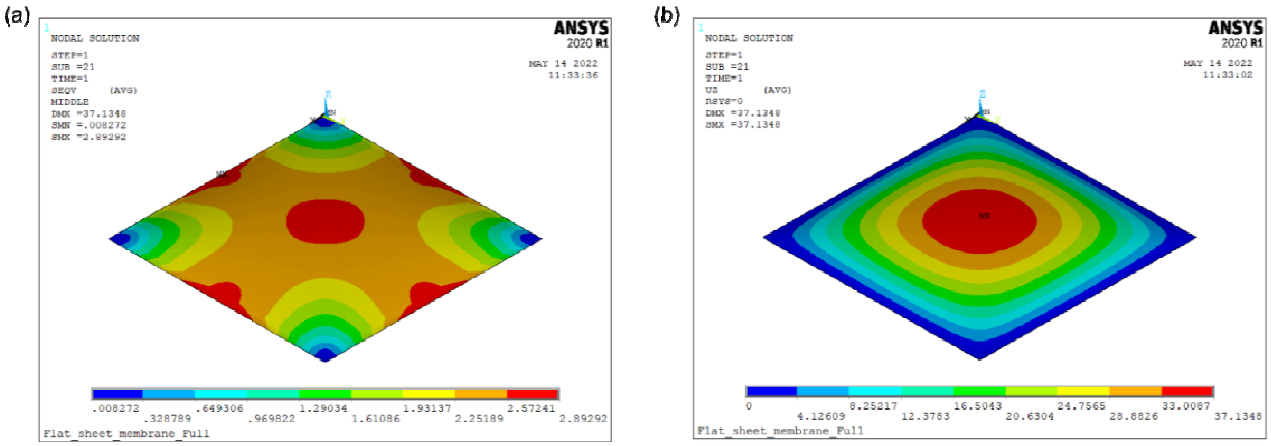

Figure 11. Backwashing results: (a) equivalent (Von Mises) stress distribution (MPa), (b) displacement component normal to the membrane surface (mm).

The maximum values of the equivalent and the first principal stresses are given in Figure 11. The maximum values of the equivalent stress and the 1st principal stresses are mostly similar; however, the 1st principal stress values slightly exceed the equivalent stress values in the case of backwashing.

The maximum values of the 1st principal stress values also suggest that the fatigue failure will likely to be controlled by the stresses occurring during the backwashing for the small and average filtration pressures, i.e., $P_f < 1.5$ bar.

At this point, it can be inferred that the membrane lives will be mainly characterized by the backwashing application for finer spacer configurations. If this is the case, allocating more spacers will not improve the overall fatigue life of the membrane.

3.2. Viscoelastic analyses

The response of the membrane sheets under the assumption of quasi-static loading has been examined in the previous section. Despite the results of the quasi-static analyses are meaningful for the assessment of the structural integrity of the viscoelastic membranes, they may not be adequate alone. It is therefore considered that the deformation of the membrane sheets under the long-term filtration pressure should be characterized.

The findings from the viscoelastic analyses could be utilized for the assessment of the permeate water quality as well as improvement of the fatigue life predictions. As described in the material modelling section, we will enforce the viscoelastic properties by means of the Prony series coefficient in ANSYS FE package [16].

A viscoelastic analysis is essentially a transient dynamic analysis without the inertia effects [21]. We therefore follow the procedure recommended in [21]. The simulation time is equal to the filtration duration, i.e., $t_{\mathrm{sim}} = 2$ h. The time increment size is set as variable based on the convergence rate of the FE simulation. The loading scheme is the one defined by Figure 3b in Section 2.1.1. The load is gradually increased up to the desired level in a short period to avoid the numerical instabilities causes by the sudden implementation of whole load in a single step.

Since the stresses acting on the membrane sheet remain more or less the same during the viscoelastic simulations, we will focus on the displacement and strain values to assess the possible decline of the permeate water quality and the compromise of the structural integrity due to the excessive deformation.

Figure 12a indicates that the maximum values of the equivalent strains for the 10×10 spacer configurations exceed the yield strain of the membrane material at almost all filtration pressure cases. We may infer that the nominal pore sizes for these cases may increase substantially, which in turn the decline of the permeate water quality might occur. On the other hand, one can readily see that the strain values for the 20×20 spacer configurations remain below the yield strain of the membrane material, which is the ideal situation for ensuring both the structural integrity and permeate water quality.

The displacement history of the membrane sheet for 10×10 configuration under the highest filtration pressure is given in Figure 12b. This figure apparently shows the viscous effects as the displacements increase continuously by the time. The maximum value of the normal displacements obtained by the quasi-static analyses in Section 3.1 is 4.32 mm, which is consistent with the displacement value for $t \cong 0$ in the viscoelastic analysis. When the simulation ends, the maximum value of the displacement becomes almost 7 mm. A similar trend can be seen for the strain components by the viscoelastic analyses.

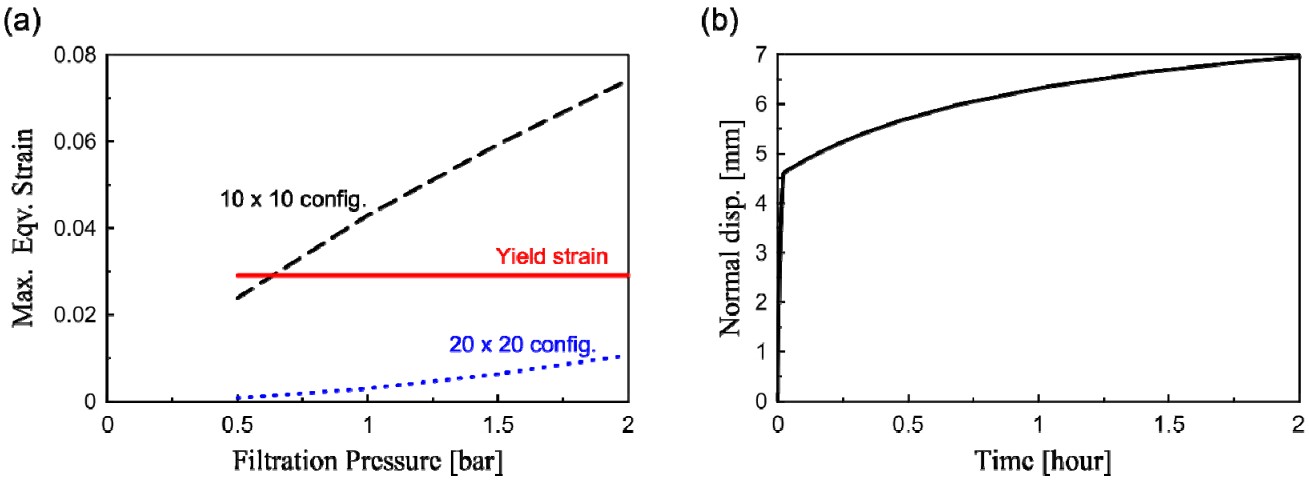

Figure 12. Viscoelastic analyses results after 2 h: (a) Maximum equivalent strain values, (b) History of displacement component normal to membrane surface for 10×10 configuration under $P_f = 2.0\ bar$.

Considering the increase of the displacements/strains under viscous effects, we will propose an approach to account for viscous deformation effects indirectly in the fatigue life predictions.

3.3. Fatigue life predictions

The procedure described in the previous section and the FE stress-strain results are utilized for the membrane mechanical life predictions. The fatigue life calculations are not performed only for the designated stress hot spots, but also they are performed for all the FE nodal points to gather damage distribution on the membranes.

The estimated mechanical fatigue lives (cycles) for the membrane sheets with and without backwashing conditions are presented in Figure 13. The without backwashing cases are demonstrated by solid black lines in Figure 13, while the fatigue lives for the filtration + backwashing cases are illustrated by the dashed red lines. The different marker types stand for the filtration pressure values. The circle "○" marker is to represent m = 0.02. The other inverse slope coefficients, m = 0.04 and 0.06 are denoted by square "□" and cross "×" markers, respectively.

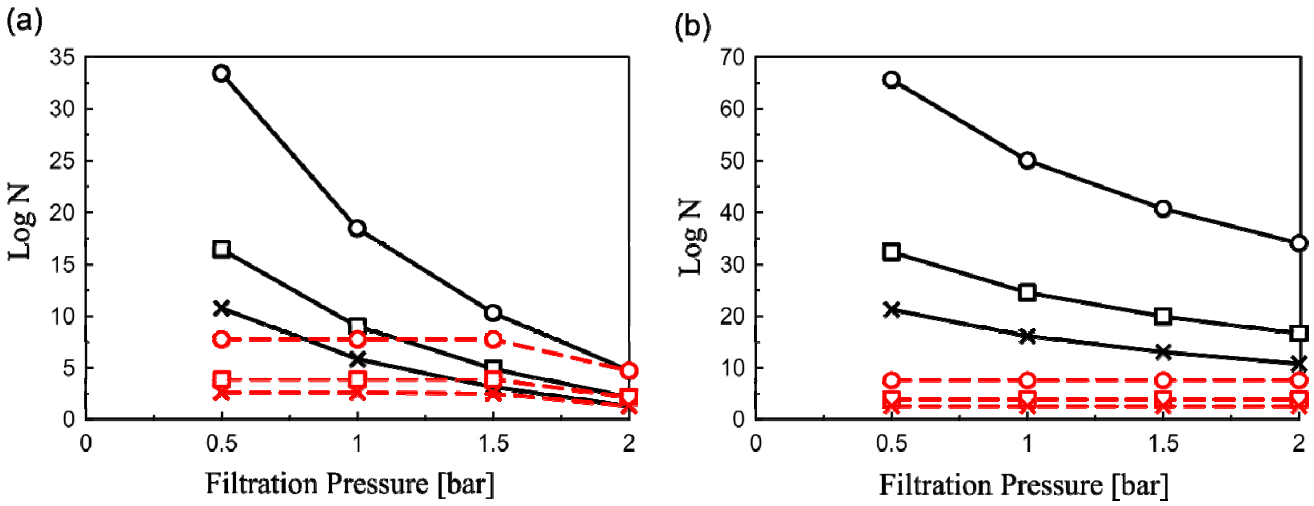

Figure 13. Fatigue life predictions: (a) 10×10 configuration, (b) 20×20 configuration.

Due to the large number of cycles in some cases, the fatigue lives are presented in the logarithmic scale in Figure 13. The fatigue cycles are then converted to *months* and presented in Tables 1 and 2. The conversion is performed by assuming each cycle, filtration + air scouring or filtration + backwashing, is about 125 min.

Table 1. Estimated mechanical fatigue lives ($month$) for flat sheet membranes with 10×10 configuration.

P_f (bar)	$m = 0.02$		$m = 0.04$		$m = 0.06$	
	Backwash	No Backwash	Backwash	No Backwash	Backwash	No Backwash
0.5	1.497E + 5	7.565E + 30	20.67	7.855E + 13	1.07	1.714E + 8
1.0	1.497E + 5	8.169E + 15	20.67	2.796E + 6	1.07	1.942E + 3
1.5	1.495E + 5	8.823E + 7	20.67	239.56	0.89	3.84
2.0	151.06	151.06	0.39	0.39	0.05	0.05

Table 2. Estimated mechanical fatigue lives ($month$) for flat sheet membranes with 20×20 configuration.

P_f (bar)	$m = 0.02$		$m = 0.04$		$m = 0.06$	
	Backwash	No Backwash	Backwash	No Backwash	Backwash	No Backwash
0.5	1.056E + 5	1.185E + 63	17.36	6.610E + 29	0.95	5.441E + 18
1.0	1.056E + 5	2.976E + 47	17.36	1.065E + 22	0.95	3.508E + 13
1.5	1.056E + 5	1.526E + 38	17.36	2.484E + 17	0.95	2.922E + 10
2.0	1.056E + 5	3.117E + 31	17.36	1.144E + 14	0.95	1.764E + 8

The fatigue life predictions for 10×10 spacer configuration are given in Table 1. As it is presented in Table 1, the backwashing operation reduces the fatigue lives dramatically. It is because of the fact that the outwards deformation of the membrane sheet under backwashing is not

constrained by the spacers. The variation of the inverse slope parameter, m, of the fatigue data impacts the estimated fatigue lives. At this point, it must be noted that the material parameters have the paramount impact on the estimated fatigue lives, and their accurate evaluation is crucial.

It is apparent that the fatigue lives of membranes become almost infinite in case of low filtration pressures without backwashing. For example, the minimum fatigue life of the membrane with 10×10 spacer configuration under $P_f = 0.5$ bar is higher than 10^{10} filtration cycles (1.714E + 8 $months$). This is partly because the environmental effects are not considered in the present work due to the lack of test data for the material under corrosive environments. It can be expected that fatigue life of the membrane will be lower than such big number in the real applications. On the other hand, it can be inferred that the fatigue failure of the membranes will be dominated by the stress cycles rather than the corrosion under higher filtration pressures, e.g., the fatigue life of membranes becomes a few hundred filtration cycles, i.e., less than a month for $P_f = 2.0$ bar. In this case, it is expected that the long-term corrosion effects will be negligible.

The fatigue life predictions for the 20×20 spacer configuration cases are presented in Table 2. The most evident observation from the table is that almost infinite life predictions for the membranes without backwashing cases. It may seem to be unrealistic; however, this outcome enables us to infer that the membrane will not fail due to the mechanical fatigue, but the main cause of the membrane failure would probably be the chemical erosion/wear of the membrane material.

The impact of the material parameter m is obvious again. If there is no backwashing implementation, the fatigue lives of the membranes become infinite even for the largest material parameter considered ($m = 0.06$). This circumstance suggests that the other material parameter C is also a significant factor impacting the membrane lives.

Since there is no available fatigue data for the considered material under corrosive environments, we have not been able to conduct fatigue simulations for the degraded membrane materials. The main material parameter that will be affected by the corrosive environment is C, which will be lower than the present value ($C = 4.438$ for intact material) in case of eroded membrane materials; however, the inverse slope of the S-N curve (m) for this material can be expected to be in the presently considered range.

In addition to the discussions above, the following observations can be articulated. If the filtration pressure is lower with backwashing, i.e., $P_f < 1.5$ bar, the fatigue lives become unchanged for the variations of the filtration pressure. This is because of the fact that the backwashing operation determines the total fatigue life, and the backwashing pressure is kept constant in this study for all filtration pressure cases. As increase of the filtration pressure, the gap between the fatigue lives for with and without backwashing cases disappears. For the highest filtration pressure case, i.e., $P_f = 2.0$ bar, the estimated fatigue lives for with and without backwashing cases are almost the same in 10×10 configurations. This situation suggests that the fatigue failure is dominated by the stresses under the filtration pressures.

Another evident observation is the gap between the fatigue lives for the membranes with different spacer configurations when the backwashing is not implemented. The stresses become significantly lower for the 20×20 configuration, and so the longer fatigue lives.

The calculated fatigue damage patterns are independent of the inverse slope coefficients, m. Then, the damage distributions for 10×10 configurations for the selected filtration pressure cases

are given in Figures 14–16 along with the colorbars representing the damage index throughout the membrane sheets. All these figures suggest that the membrane failures occur along the framing region due to the higher stresses. It is also obvious from these figures that the impact of filtration pressure becomes visible on the damage patterns for the backwashing cases.

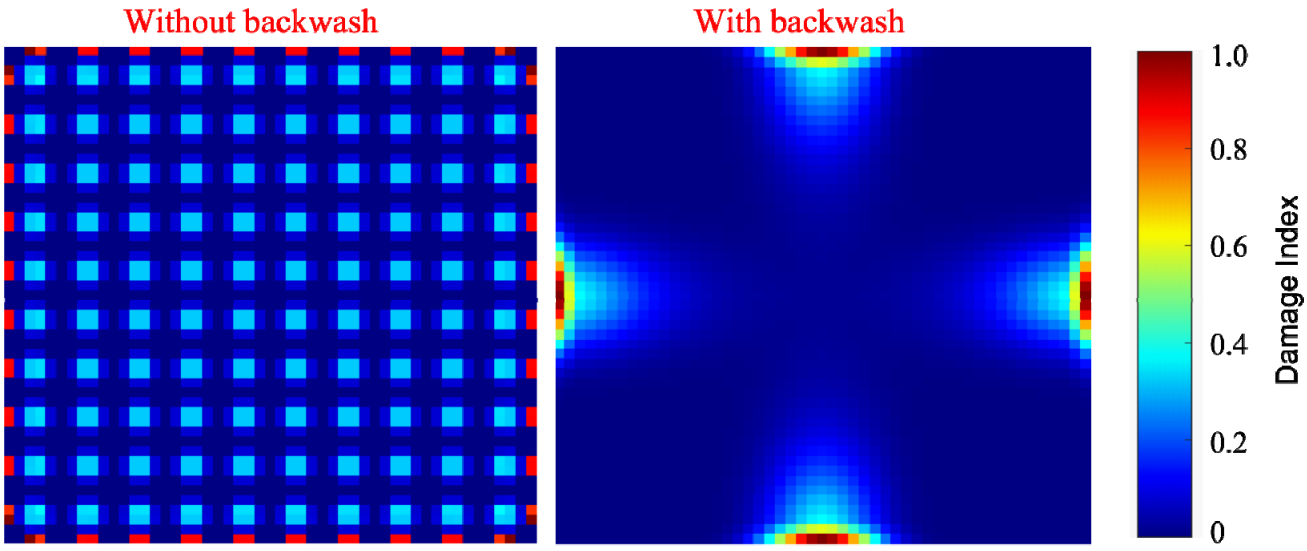

Figure 14. Accumulated damage patterns for 10×10 configuration under filtration pressure, $P_f = 0.5\ bar$.

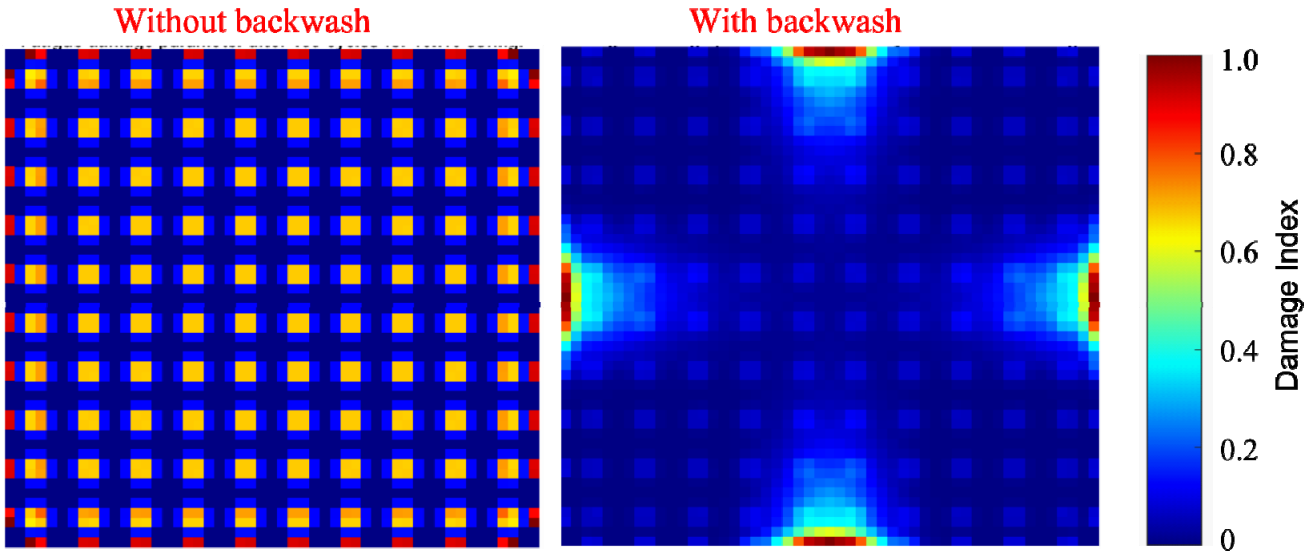

Figure 15. Accumulated damage patterns for 10×10 configuration under filtration pressure, $P_f = 1.5\ bar$.

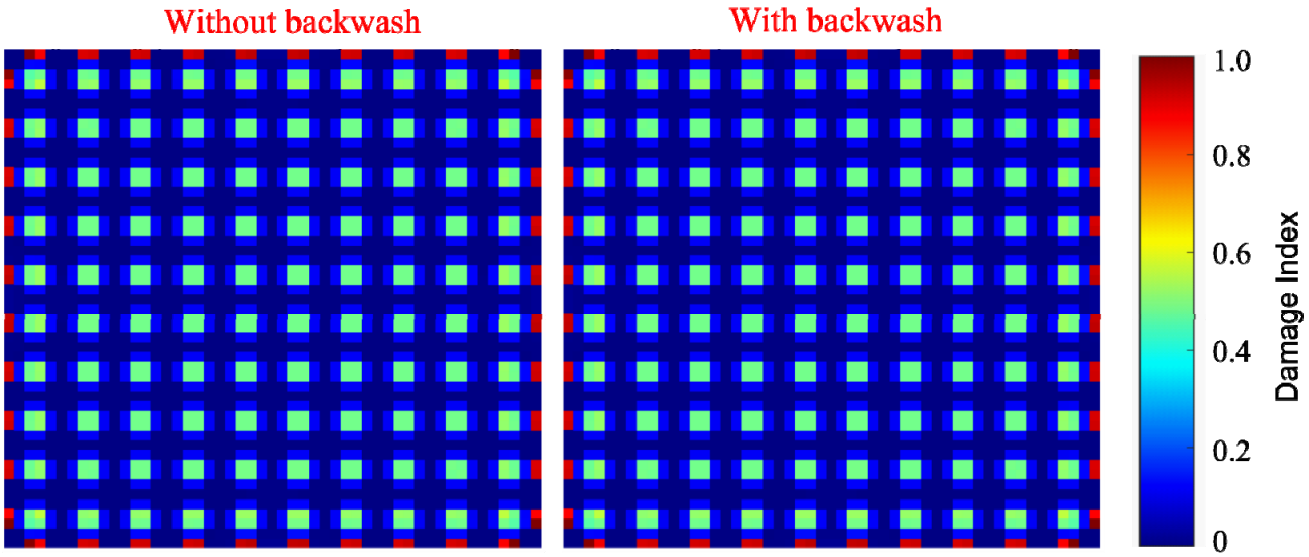

Figure 16. Accumulated damage patterns for 10×10 configuration under filtration pressure, $P_f = 2.0\ bar$.

The accumulated damage patterns for 20×20 configurations are almost the same regardless of the considered filtration pressure values. If the backwashing is applied, the failure takes places on the mid-edges of the sheet because of the backwashing deformations in all filtration cases, see Figure 17. If the backwashing is not the case, the membrane lives becomes almost infinite, see Figure 13b; and the fatigue damage accumulates at the corner points, see Figure 17.

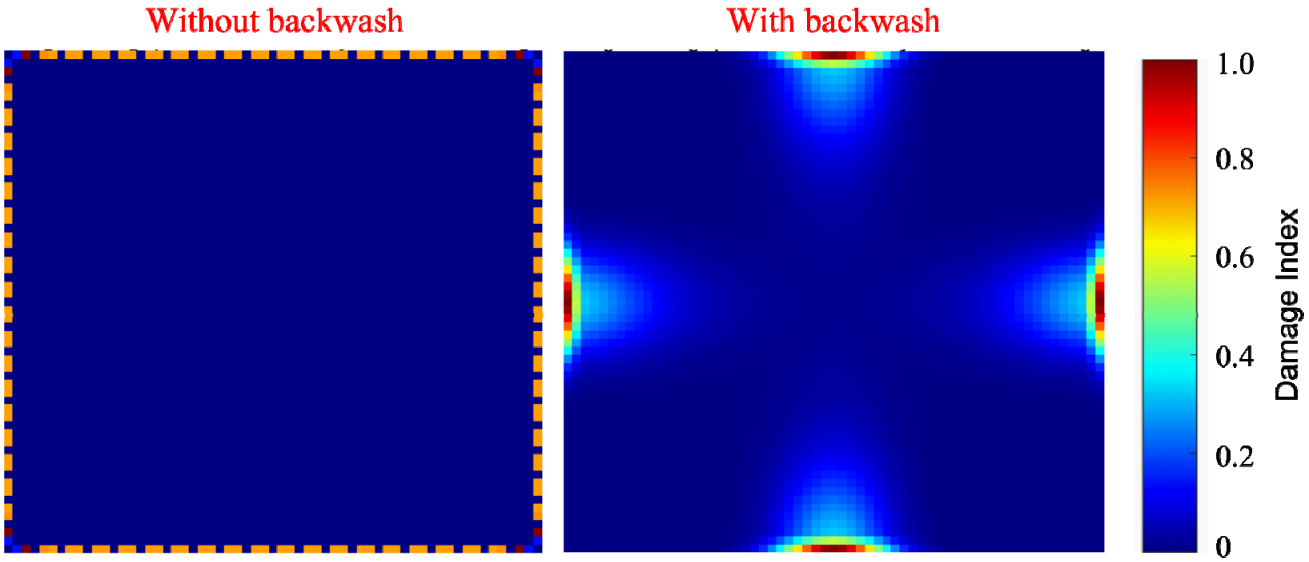

Figure 17. Accumulation of damage patterns for 20×20 spacer configurations.

4. Conclusions

A procedure for assessing the mechanical response and fatigue life of flat-sheet water treatment

membranes has been presented. Then, the procedure has been demonstrated by an extensive study on the water treatment membranes. The proposed procedure is applicable for any thickness values of flat-sheet membranes. The main assumptions in the proposed methodology as well as the observations are summarized as follows.

The spacers are assumed to support the membranes under filtration, but the mechanical support of the spacers under backwashing is omitted as the flow direction is reverse and the membrane sheet deforms outwards.

Long-term viscoelastic analyses have revealed that the equivalent strains for 10×10 spacer configurations exceed the yield strain of the membrane material in the most filtration cases. This situation is expected to compromise the permeate water quality.

We have proposed a simplified approach to account for the long-term deformation effects of the viscoelastic membranes in the mechanical fatigue life predictions. Fatigue failure damage of the membrane sheets are accumulated along the framing lines for all cases.

The membrane sheets with 20×20 spacer configurations mostly remain mechanically safe as long as the backwashing is not implemented. In the 20×20 spacer configurations, the membrane failure is dominated by the backwashing regardless of the filtration pressure. The assumption on the mechanical support of the spacers under backwashing pressure is a conservative approach, if a special configuration can be adopted to support membrane deformation under backwashing, the membrane lives can be improved significantly.

On the other hand, it is possible to observe the impact of filtration pressure on the fatigue damage accumulation for 10×10 spacer configurations, particularly for $P_f \geq 1.5\, bar$.

In summary, the proposed procedure has been demonstrated through the case studies, and the main observation from the cases studies is that the membrane sheets become mechanically safe when the filtration pressure is $P_f \leq 1.5\,\text{bar}$ and the backwashing is not implemented for the considered membrane sheet properties and spacer configurations. The proposed procedure can also be employed for the long-term fatigue life predictions under corrosive environment with the proper material data representing the actual conditions.

Acknowledgements

This work was supported by an Institutional Links grant, ID 527426826, under the Egypt-Newton-Mosharafa Fund partnership. The grant is funded by the UK Department for Business, Energy and Industrial Strategy and Science, Technology and Innovation Funding Authority (STIFA)-project NO. 42717 (An Integrated Smart System of Ultrafiltration, Photocatalysis, Thermal Desalination for Wastewater Treatment) and delivered by the British Council.

Conflict of interest

The authors have no conflicts of interest to declare.

References

1. Judd S (2010) MBR Book, 2Eds., Oxford: Butterworth-Heinemann.
2. Madaeni SS, Ghaemi N, Rajabi H (2015) Advances in polymeric membranes for water treatment, *Advances in Membrane Technologies for Water Treatment*, Cambridge: Woodhead Publishing, 3–41.
3. Childress AE, Le-Clech P, Daugherty JL, et al. (2005) Mechanical analysis of hollow fiber membrane integrity in water reuse applications. *Desalination* 180: 5–14.
4. Wang K, Abdalla AA, Khaleel MA, et al. (2017) Mechanical properties of water desalination and wastewater treatment membranes. *Desalination* 401: 190–205.
5. Ejaz Ahmed F, Lalia B, Hilal N, et al. (2014) Underwater superoleophobic cellulose/electrospun PVDF-HFP membranes for efficient oil/water separation. *Desalination* 344: 48–54.
6. Hou D, Wang J, Sun X, et al. (2012) Preparation and properties of PVDF composite hollow fiber membranes for desalination through direct contact membrane distillation. *J Membrane Sci* 405: 185–200.
7. Hong J, He Y (2012) Effects of nano sized zinc oxide on the performance of PVDF microfiltration membranes. *Desalination* 302: 71–79.
8. Chartoff RP, Menczel JD, Dillman SH (2008) Dynamic mechanical analysis (DMA), In: Menczel JD, Prime RB, *Thermal Analysis of Polymers: Fundamentals and Applications*, John Wiley & Sons.
9. Chung TS, Qin JJ, Gu J (2000) Effect of shear rate within the spinneret on morphology, separation performance and mechanical properties of ultrafiltration polyethersulfone hollow fiber membranes. *Chem Eng Sci* 55: 1077–1091.
10. Lalia BS, Guillen-Burrieza E, Arafat HA, et al. (2013) Fabrication and characterization of polyvinylidenefluoride-co-hexafluoropropylene (PVDF-HFP) electrospun membranes for direct contact membrane distillation. *J Membrane Sci* 428: 104–115.
11. Mackin TJ, Vernon PJ, Matthew RB (2004) Fatigue testing of polymer membranes. *Polym Composite* 25: 442–450.
12. Hartinger M, Napiwotzki J, Schmid EM, et al. (2020) Influence of spacer design and module geometry on the filtration performance during skim milk microfiltration with flat sheet and spiral-wound membranes. *Membranes* 10: 57.
13. Aerts PEM, Backwash efficiency in IPC® membrane modules for MBR, 2019. Available from: https://www.linkedin.com/pulse/backwash-efficiency-ipc-membrane-modules-mbr-peter-e-m-aerts/.
14. ANSYS Inc, 2018. ANSYS mechanical APDL basic analysis guide.
15. Emori K, Miura T, Kishida H, et al. (2019) Creep deformation behavior of polymer materials with a 3D random pore structure: Experimental investigation and FEM modeling. *Polym Test* 80: 106097.
16. ANSYS Inc., 2018. ANSYS mechanical APDL material reference.
17. MATLAB, Curve Fitting Toolbox. Mathworks, 2022. Available from: https://uk.mathworks.com/products/curvefitting.html.

18. Tng KH (2018) Mechanical failure in potable reuse plants: Component and system relibality considerations [PhD Thesis]. University of New South Wales, Sydney.
19. Solvay, 2018. Solef PVDF design and processing guide. Solef-PVDF-Design-and-Processing-Guide_EN-v2.7_0.pdf
20. Fane AG (2008) Submerged membranes, *Advanced Membrane Technology and Applications*, New Jersey: Jonh Wiley & Sons, 239–270.
21. ANSYS Inc., 2018. ANSYS mechanical APDL structural analysis guide.